CONFIDENTIAL

NACA

RESEARCH MEMORANDUM

AERODYNAMIC CHARACTERISTICS OF A DELTA WING WITH LEADING EDGE SWEPT BACK 45°, ASPECT RATIO 4, AND NACA 65A006 AIRFOIL SECTION

TRANSONIC-BUMP METHOD

By William C. Sleeman, Jr., and Robert E. Becht

Langley Aeronautical Laboratory
Langley Air Force Base, Va.

NATIONAL ADVISORY COMMITTEE FOR AERONAUTICS

WASHINGTON

September 6, 1949

CONFIDENTIAL

NATIONAL ADVISORY COMMITTEE FOR AERONAUTICS

RESEARCH MEMORANDUM

AERODYNAMIC CHARACTERISTICS OF A DELTA WING WITH LEADING EDGE SWEPT BACK 45°, ASPECT RATIO 4, AND NACA 65A006 AIRFOIL SECTION

TRANSONIC-BUMP METHOD

By William C. Sleeman, Jr., and Robert E. Becht

SUMMARY

As part of an NACA transonic research program, a series of wing-body combinations are being investigated in the Langley high-speed 7- by 10-foot tunnel over a Mach number range from 0.60 to 1.18 utilizing the transonic-bump test technique.

This paper presents the results of the investigation of a wing-alone and wing-fuselage combination employing a delta wing having 45° sweepback of the leading edge, aspect ratio 4, and an NACA 65A006 airfoil section. Lift, drag, pitching moment, and root bending moment were obtained for these configurations. In addition, effective downwash angles and dynamic-pressure characteristics in the region of a probable tail location also were obtained for these configurations, and are presented for a range of tail heights at one tail length. In order to expedite publishing of these data, only a brief analysis is included.

INTRODUCTION

A series of wing-body configurations are being investigated in the Langley high-speed 7- by 10-foot tunnel to study the effects of wing geometry on the longitudinal stability characteristics at transonic speeds. A Mach number range between 0.60 and 1.18 is obtained utilizing the transonic-bump test technique. Previous data published in this series are presented in references 1 to 4.

This paper presents the results of the investigation of the wing-alone and wing-fuselage configurations employing a delta wing with 45° sweepback of the leading edge, aspect ratio of 4, and an NACA 65A006 airfoil section.

MODEL AND APPARATUS

The wing of the semispan delta-wing model had 45° sweepback of the leading edge, aspect ratio 4, and an NACA 65A006 airfoil section parallel to the free stream. The wing was made of beryllium copper and fuselage of brass. A two-view drawing of the model is presented in figure 1 while ordinates of the fuselage of fineness ratio 10 are given in table I. End plates, $\frac{1}{32}$ inch thick, were used on all configurations.

The model was mounted on an electrical strain-gage balance, which was enclosed in the bump; and the lift, drag, pitching moment, and bending moment about the model plane of symmetry were measured with calibrated galvanometers.

Effective downwash angles were determined for a range of tail heights by measuring the floating angles of five free-floating tails with the aid of calibrated slide-wire potentiometers. Details of the floating tails are shown in figures 2 and 3, while a photograph of the test setup on the bump, showing the floating tail mounted in the fuselage, is given in figure 4. The tails used in this investigation were the same as those used in the investigations reported in references 1 to 4.

A total-head rake was used to determine dynamic-pressure ratios for a range of tail heights along a line containing the 25-percent mean-aerodynamic-chord point of the free-floating tails. The total-head tubes were spaced 0.125 inch apart for a distance of 1 inch below and 0.5 inch above the wing chord plane extended ($\alpha = 0$) and were 0.25 inch apart for the remainder of the rake.

SYMBOLS

C_L lift coefficient $\left(\frac{\text{Twice panel lift}}{qS}\right)$

C_D drag coefficient $\left(\frac{\text{Twice panel drag}}{qS}\right)$

C_m pitching-moment coefficient referred to $0.25\bar{c}$ $\left(\frac{\text{Twice panel pitching moment}}{qS\bar{c}}\right)$

C_B bending-moment coefficient about root chord line (at plane of symmetry) $\left(\frac{\text{Root bending moment}}{q\frac{S}{2}\frac{b}{2}}\right)$

q effective dynamic pressure over span of model, pounds per square foot $\left(\frac{1}{2}\rho V^2\right)$

S twice wing area of semispan model, 0.1250 square foot

$\bar{c}$ mean aerodynamic chord of wing, 0.2357 foot; based on relationship $\frac{2}{S}\int_0^{b/2} c^2 dy$

c local wing chord

b twice span of semispan model

y spanwise distance from plane of symmetry

ρ air density, slugs per cubic foot

V free-stream velocity, feet per second

M effective Mach number over span of model

M_l local Mach number

M_a average chordwise local Mach number

R Reynolds number of wing based on $\bar{c}$

α angle of attack, degrees

ϵ effective downwash angle, degrees

q_{wake}/q ratio of point dynamic pressure taken along a line containing the quarter-chord points of the mean aerodynamic chords of the free-floating tails to local free-stream dynamic pressure

$y_{c.p.}$ lateral center of pressure, percent semispan $\left(100C_B/C_L\right)$

h_t tail height relative to wing chord plane extended, percent semispan, positive for tail positions above chord plane extended

a.c. aerodynamic center

TESTS

The tests were conducted in the Langley high-speed 7- by 10-foot tunnel utilizing an adaptation of the NACA wing-flow technique for obtaining transonic speeds. The technique used involves the mounting of a model in the high-velocity flow field generated over the curved surface of a bump located on the tunnel floor. (See reference 5.)

Typical contours of local Mach number in the vicinity of the model location on the bump obtained from surveys with no model in position are shown in figure 5. It is seen that there is a Mach number gradient which results in a difference in Mach number of about 0.05 over the model semispan at low Mach numbers and from 0.06 to 0.07 at the highest Mach numbers. The chordwise Mach number generally varies less than 0.01. No attempt has been made to evaluate the effects of this chordwise and spanwise Mach number variation. Note that the long-dashed lines shown near the root of the wing (fig. 5) represent a local Mach number 5 percent below the maximum value and indicate a nominal extent of the bump boundary layer. The effective test Mach number was obtained from contour charts similar to those presented in figure 5 using the relationship

$$M = \frac{2}{S}\int_0^{b/2} cM_a\,dy$$

The variation of mean test Reynolds number with Mach number is shown in figure 6. The boundaries in the figure indicate the range in Reynolds number caused by variations in test conditions in the course of the investigation.

Force and moment data, effective downwash angles, and the ratio of dynamic pressure at 25 percent of the tail mean aerodynamic chord to free-stream dynamic pressure were obtained for the model configurations through a Mach number range of 0.60 to 1.18 and an angle-of-attack range of -2° to 10°.

No tares have been applied to the data to account for the presence of the end plates on the models. Jet-boundary corrections have not been evaluated because the boundary conditions to be satisfied are not rigorously defined. However, inasmuch as the effective flow field is large compared with the span and chord of the model, the corrections are believed to be small.

By measuring tail floating angles without a model installed, it was determined that a tail spacing of 2 inches would produce negligible interference effects of reflected shock waves on the tail floating angles. Downwash angles for the wing-alone configuration were therefore obtained simultaneously for the middle, highest, and lowest tail positions in one series of tests and simultaneously for the two intermediate positions in succeeding runs. (See fig. 3.) For the wing-fuselage tests, the effective downwash angles at the wing chord plane extended were determined by mounting a free-floating tail on the center line of the fuselage. The downwash angles presented are increments from the tail floating angles without a model in position. It should be noted that the floating angles measured are in reality a measure of the angle-of-zero pitching moment about the tail pivot axis rather than the angle-of-zero lift. It has been estimated, however, that for the tail arrangement used a downwash gradient of 2° across the span of the tail will result in an error of less than 0.2° in the measured downwash angle.

Total-head readings obtained from the tail survey rake have been corrected for bow-wave loss. The static-pressure values used in computing the dynamic-pressure ratios were obtained by use of a static probe with no model in position.

RESULTS AND DISCUSSION

A table of the figures presenting the results is given below:

	Figure
Wing-alone force data	7
Wing-fuselage force data	8
Effective downwash angles (wing alone)	9
Effective downwash angles (wing fuselage)	10
Downwash gradients	11
Dynamic-pressure surveys	12
Summary of aerodynamic characteristics	13

The discussion is based on the summarized values given in figure 13 unless otherwise noted. The slopes summarized in figure 13 have been averaged over a range of ± 0.1 of the stated lift coefficient.

Lift and Drag Characteristics

The lift-curve slope measured near zero lift for the wing alone was approximately 0.064 at a Mach number of 0.60. The experimental slope agrees with the value estimated by use of the charts in reference 6 for 0.60 Mach number. The addition of the fuselage had essentially no effect on the lift-curve slope up to a Mach number of 1.00 but increased the lift-curve slope at Mach numbers above M = 1.00. At a Mach number of 1.15 the fuselage increased the lift-curve slope about 11 percent.

The drag rise at zero lift began at a Mach number of about 0.92 for both the wing-alone and wing-fuselage configurations. The absolute drag coefficients are probably high because of the presence of the end plates and the relatively low Reynolds numbers at which these tests were made.

The lateral center of pressure for the wing alone $\left(C_L = 0.3\right)$ was located at 40 percent of the semispan at a Mach number of 0.6. This value compares with an estimated low-speed value of 40.3 percent semispan. (See reference 6.) Between M = 0.9 and 1.00 a fairly abrupt movement of $y_{c.p.}$ to about 45 percent semispan occurred. The addition of the fuselage had no effect at low Mach numbers but moved $y_{c.p.}$ inboard approximately 2 percent semispan above a Mach number of 0.95.

Pitching-Moment Characteristics

At low Mach numbers the aerodynamic-center location near zero lift for the wing alone was 41 percent of the mean aerodynamic chord $\left(\left(\frac{\partial C_m}{\partial C_L}\right)_M = -0.16\right)$. The estimated low-speed aerodynamic-center location (reference 6) was 33 percent of the mean aerodynamic chord. The effect of the fuselage on the stability at low lift coefficients was slightly destabilizing up to a Mach number of 1.00. Above M = 1.00 the fuselage produced a slight stabilizing effect.

In the subsonic-speed range the wing-alone and wing-fuselage pitching-moment curves indicated a destabilizing trend at higher lift coefficients. (See figs. 7 and 8.) This effect is characteristic of wings with appreciable sweepback. However, above M = 1.00 there is no indication of this destabilizing trend even at the highest lift coefficients attained. Similar trends in pitching-moment characteristics were found in the results presented in references 1 to 4.

Downwash and Dynamic-Pressure Surveys

The variation of effective downwash angle with tail height and angle of attack for the wing-alone and wing-fuselage configurations at various Mach numbers is presented in figures 9 and 10. The downwash gradient $\partial\epsilon/\partial\alpha$ near zero lift for the wing alone (fig. 11) increased as the tail location approached the chord plane. This trend in $\partial\epsilon/\partial\alpha$ was evidenced throughout the Mach number range tested. At higher lift coefficients, $\partial\epsilon/\partial\alpha$ was generally less than the zero-lift value for tail positions below the chord plane and was higher for tail positions above the chord plane (figs. 9 and 10). The addition of the fuselage caused only small changes in the downwash gradients.

Note that the test angle-of-attack range with the free-floating tail slightly below the chord plane extended was restricted by the presence of the fuselage.

The results of point-dynamic-pressure surveys made along a line containing the 25-percent mean-aerodynamic-chord points of the free-floating tails used in the downwash surveys are presented in figure 12. The maximum loss in dynamic pressure at the wake center line for high angles of attack increased with Mach number from 23 percent ($M = 0.70$) to 30 percent ($M = 1.15$) of the free-stream dynamic pressure. The width of the wake also became somewhat greater at higher Mach numbers.

The addition of the fuselage showed only a small effect on the wake profiles although the peak losses were reduced in some cases.

Langley Aeronautical Laboratory
National Advisory Committee for Aeronautics
Langley Air Force Base, Va.

REFERENCES

1. Weil, Joseph, and Goodson, Kenneth W.: Aerodynamic Characteristics of a Wing with Quarter-Chord Line Swept Back 45°, Aspect Ratio 4, Taper Ratio 0.6, and NACA 65A006 Airfoil Section. Transonic-Bump Method. NACA RM L9A21, 1949.

2. Sleeman, William C., Jr., and Becht, Robert E.: Aerodynamic Characteristics of a Wing with Quarter-Chord Line Swept Back 35°, Aspect Ratio 4, Taper Ratio 0.6, and NACA 65A006 Airfoil Section. Transonic-Bump Method. NACA RM L9B25, 1949.

3. Myers, Boyd C., II, and King, Thomas J., Jr.: Aerodynamic Characteristics of a Wing with Quarter-Chord Line Swept Back 45°, Aspect Ratio 4, Taper Ratio 0.3, and NACA 65A006 Airfoil Section. Transonic-Bump Method. NACA RM L9E25, 1949.

4. King, Thomas J., Jr., and Myers, Boyd C., II.: Aerodynamic Characteristics of a Wing with Quarter-Chord Line Swept Back 60°, Aspect Ratio 4, Taper Ratio 0.6, and NACA 65A006 Airfoil Section. Transonic-Bump Method. NACA RM L9G27, 1949.

5. Schneiter, Leslie E., and Ziff, Howard L.: Preliminary Investigation of Spoiler Lateral Control on a 42° Sweptback Wing at Transonic Speeds. NACA RM L7F19, 1947.

6. DeYoung, John: Theoretical Additional Span Loading Characteristics of Wings with Arbitrary Sweep, Aspect Ratio, and Taper Ratio. NACA TN 1491, 1947.

TABLE I.- FUSELAGE ORDINATES

[Basic fineness ratio 12; actual fineness ratio 10 achieved by cutting off the rear one-sixth of the body; $\bar{c}/4$ located at $l/2$]

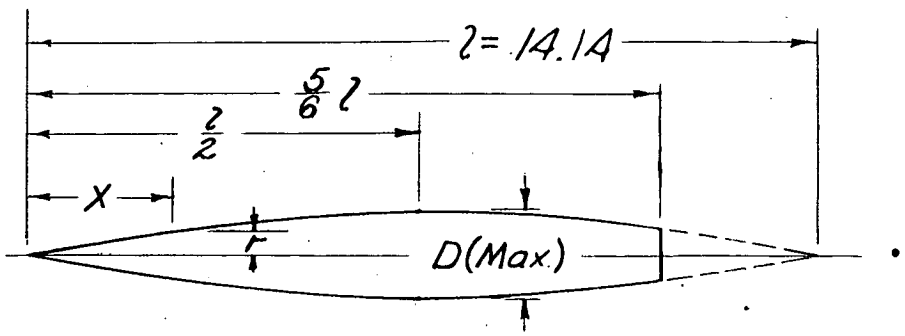

Ordinates			
x/l	r/l	x/l	r/l
0	0	0	0
.005	.00231	.4500	.04143
.0075	.00298	.5000	.04167
.0125	.00428	.5500	.04130
.0250	.00722	.6000	.04024
.0500	.01205	.6500	.03842
.0750	.01613	.7000	.03562
.1000	.01971	.7500	.03128
.1500	.02593	.8000	.02526
.2000	.03090	.8338	.02000
.2500	.03465	.8500	.01852
.3000	.03741	.9000	.01125
.3500	.03933	.9500	.00439
.4000	.04063	1.0000	0
L. E. radius = 0.0005l			

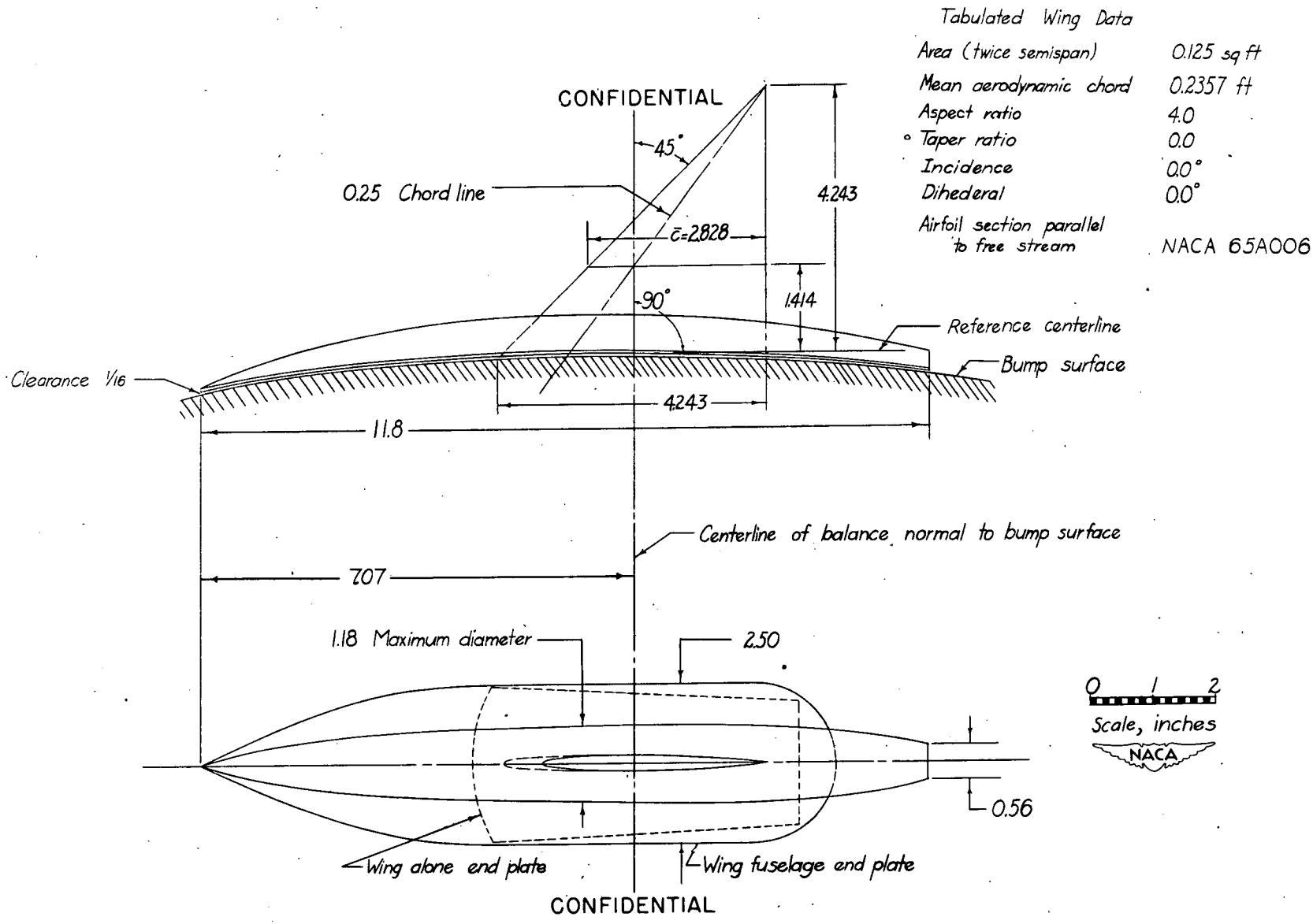

Figure 1.– General arrangement of delta–wing model with leading edge swept back 45°, aspect ratio 4, and NACA 65A006 airfoil.

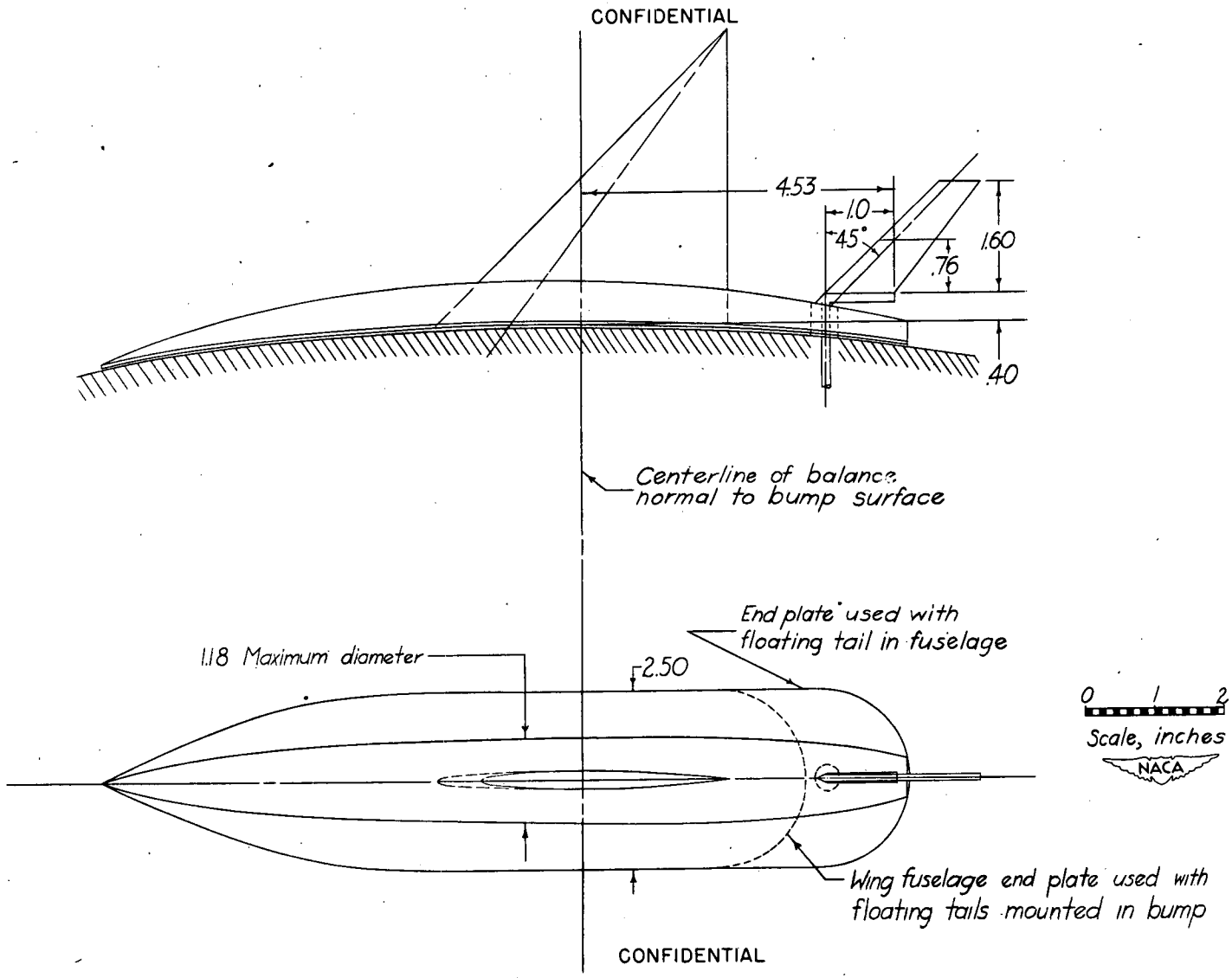

Figure 2.— Details of free-floating tail mounted in fuselage of delta-wing model with leading edge swept back 45°, aspect ratio 4, and NACA 65A006 airfoil.

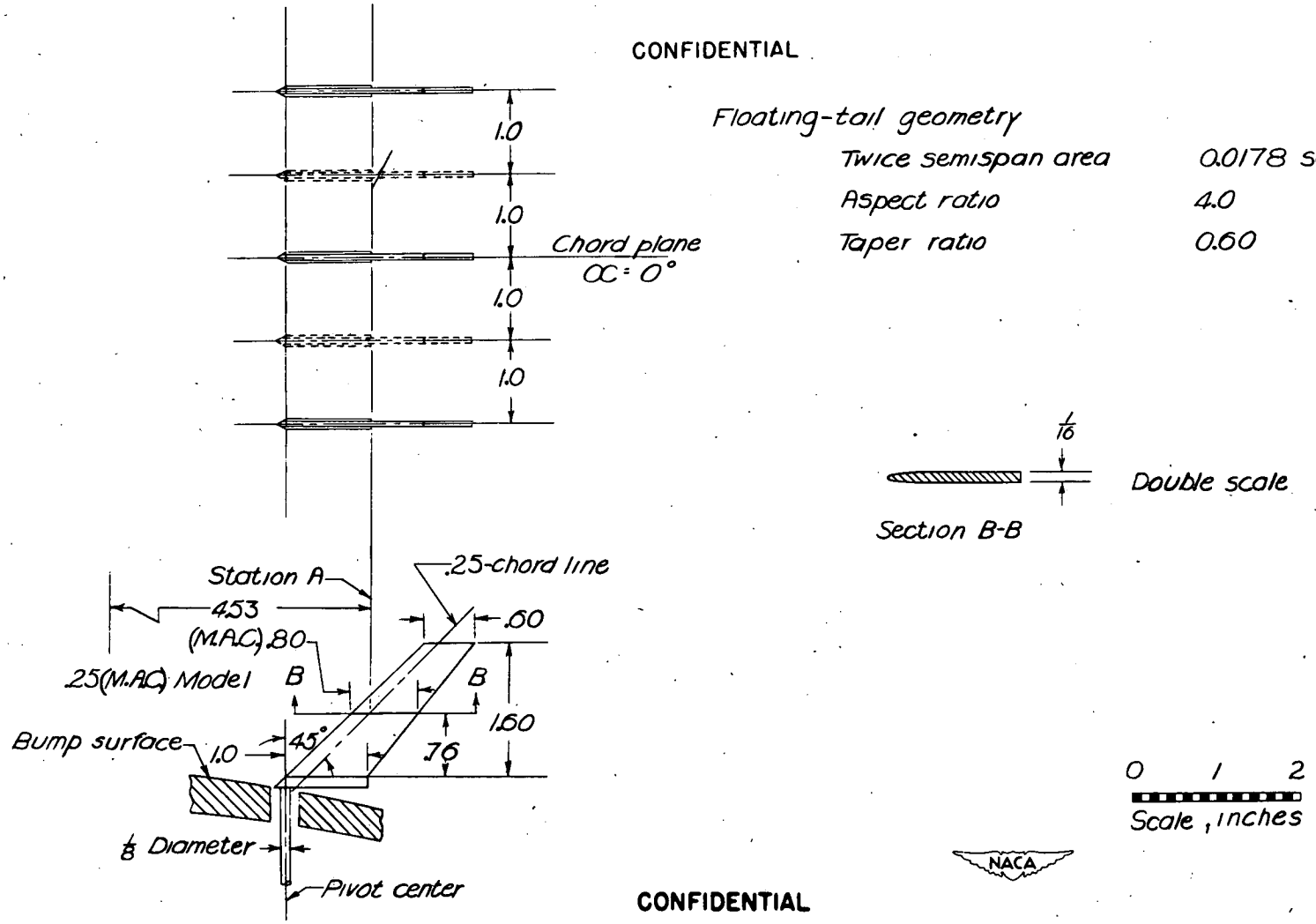

Figure 3.– Details of free-floating tails used in downwash surveys behind delta-wing model with leading-edge swept back 45°, aspect ratio 4, and NACA 65A006 airfoil.

CONFIDENTIAL

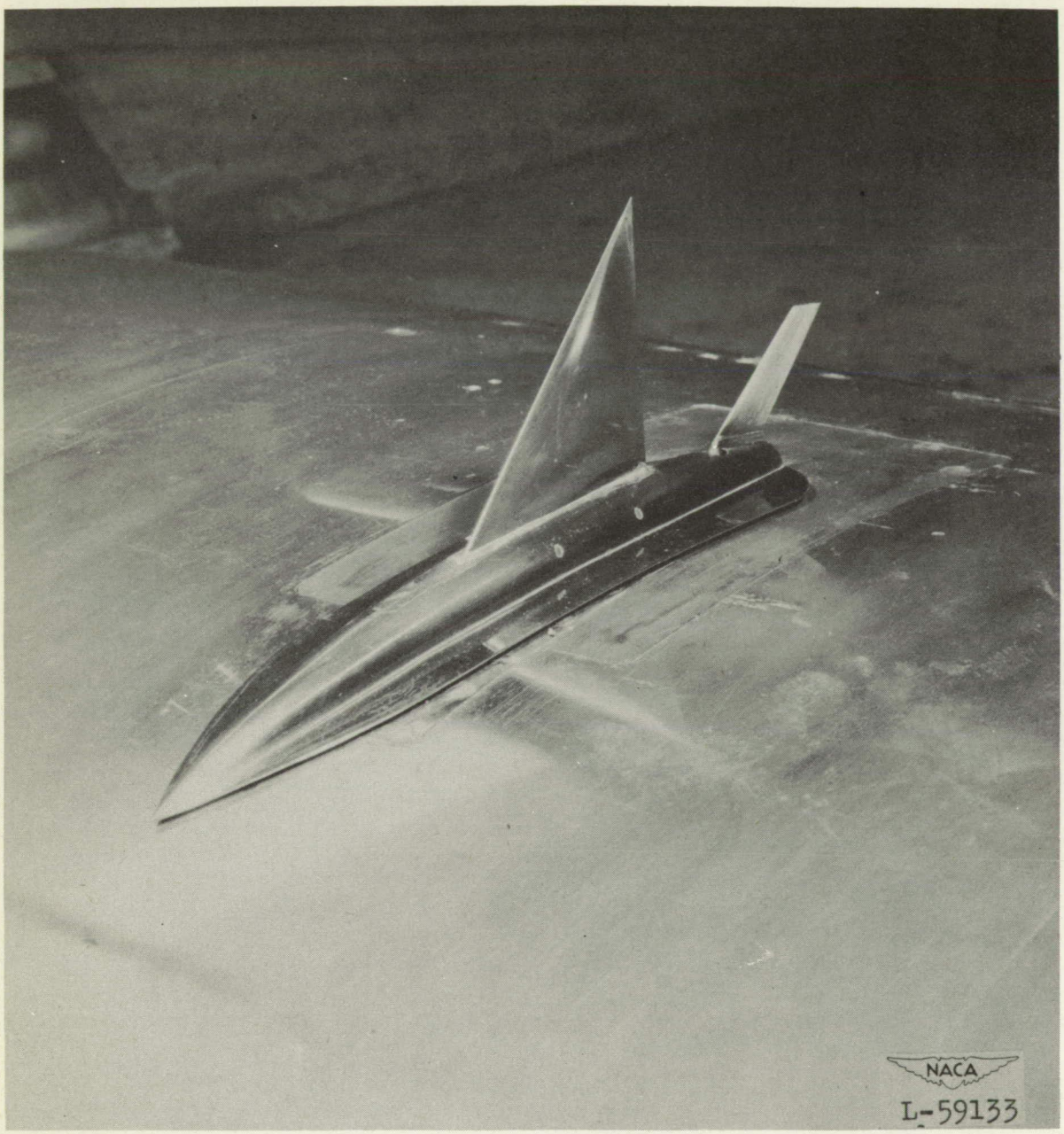

Figure 4.– Photograph of delta–wing model with leading edge swept back 45°, aspect ratio 4, and NACA 65A006 airfoil showing free–floating tail mounted in fuselage.

CONFIDENTIAL

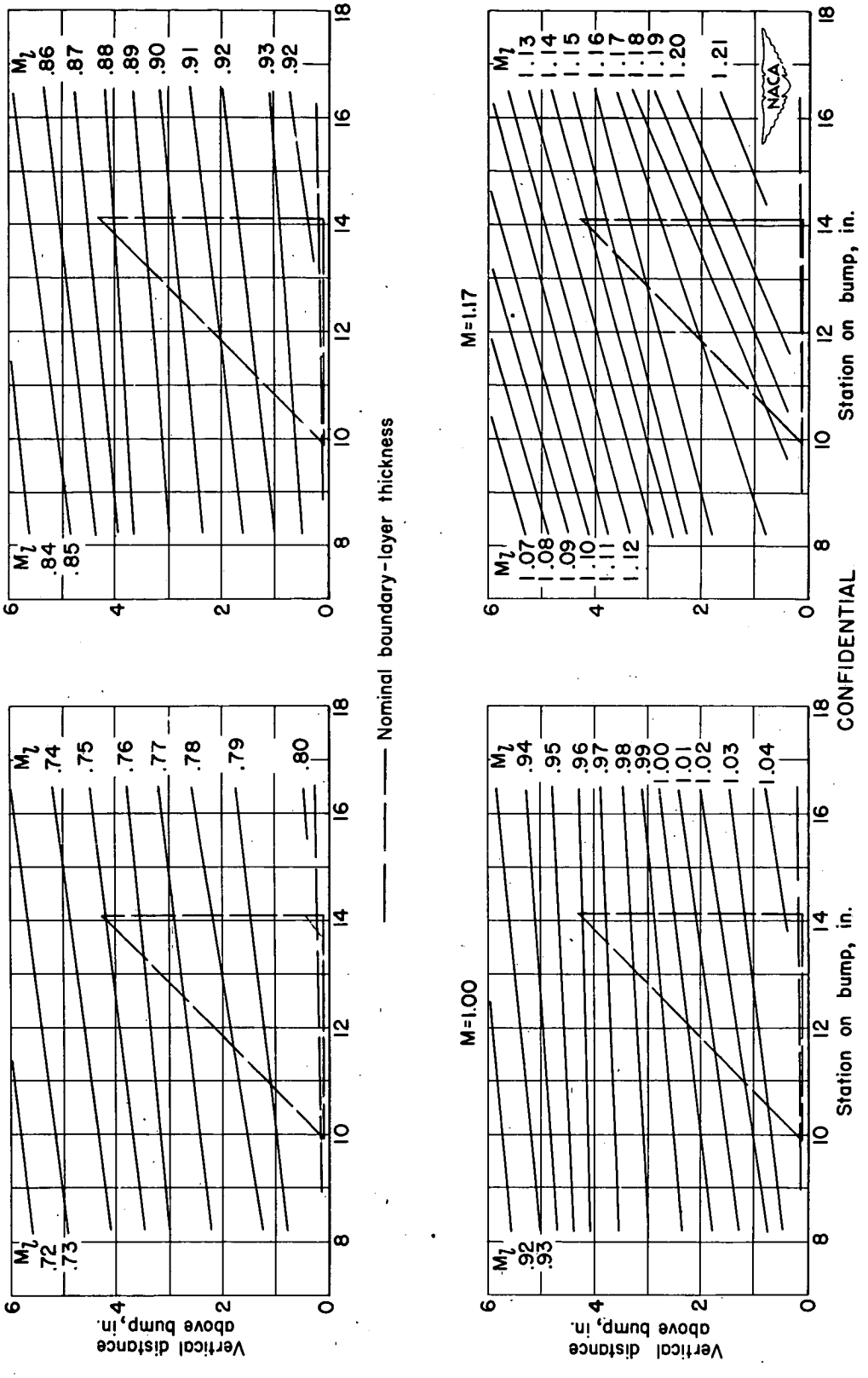

Figure 5.- Typical Mach number contours over transonic bump in region of model location.

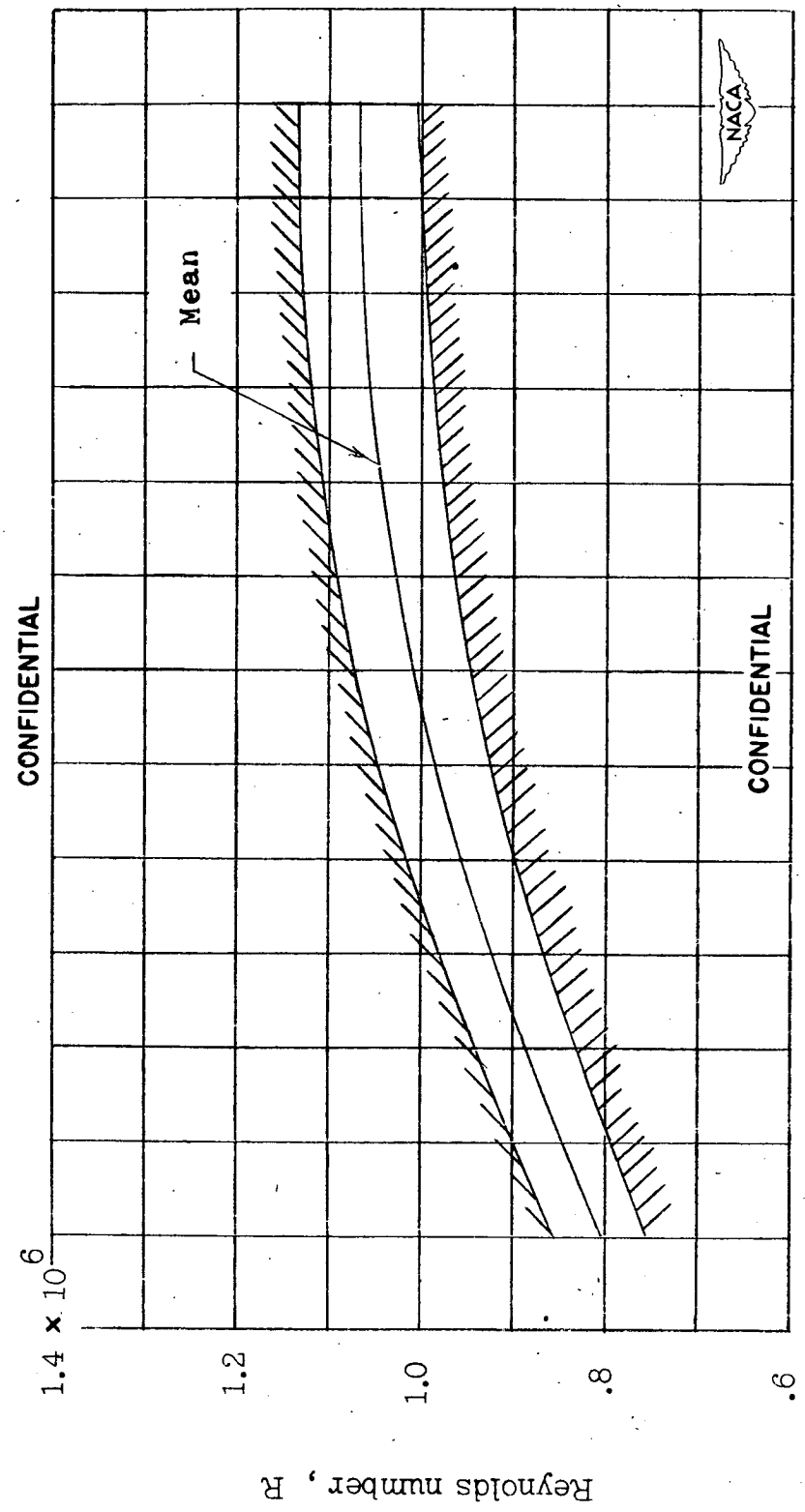

Figure 6.- Variation of test Reynolds number with Mach number for delta-wing model with leading edge swept back 45°, aspect ratio 4, and NACA 65A006 airfoil.

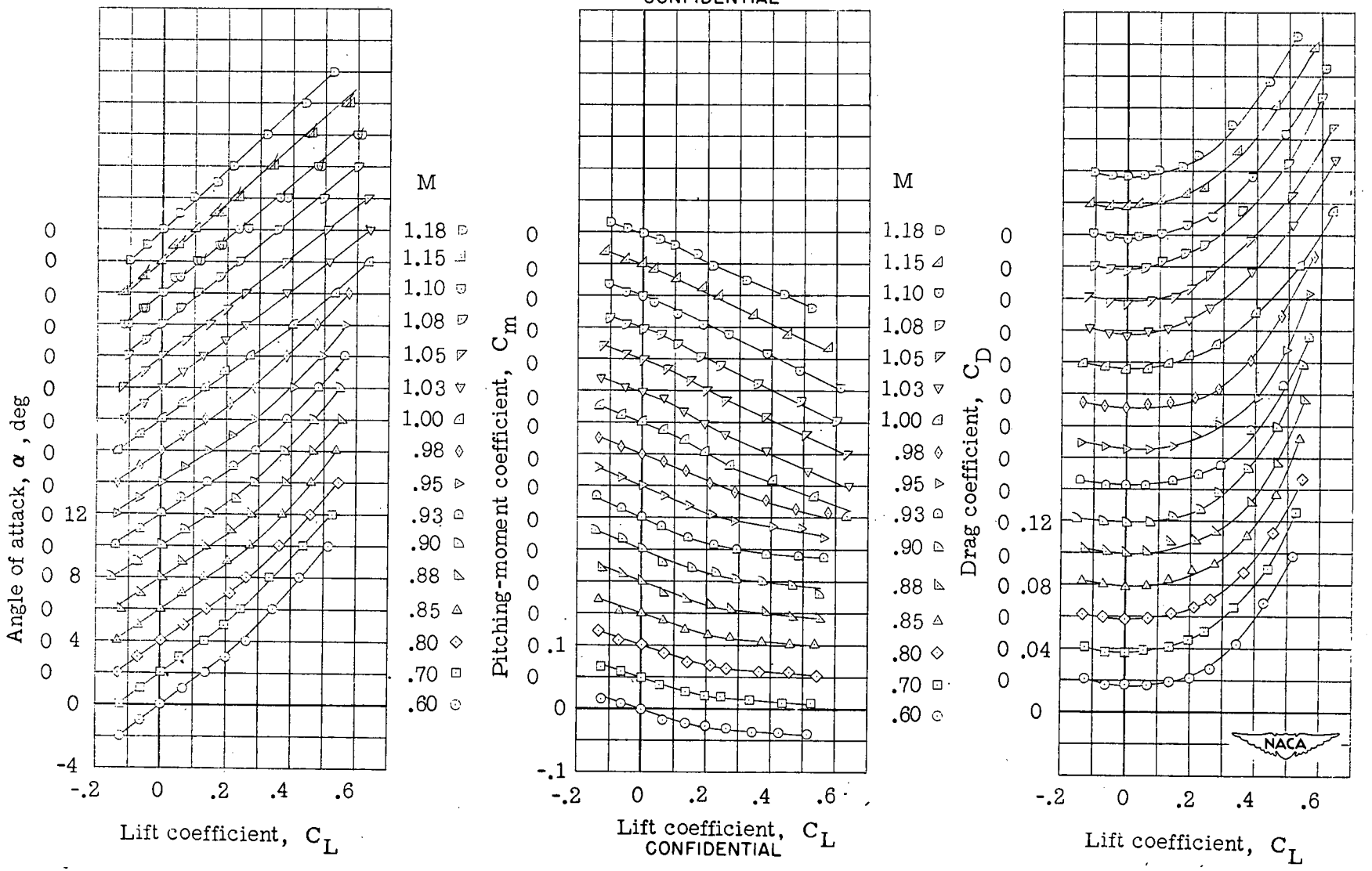

Figure 7.– Wing–alone aerodynamic characteristics for delta–wing model with leading edge swept back 45°, aspect ratio 4, and NACA 65A006 airfoil.

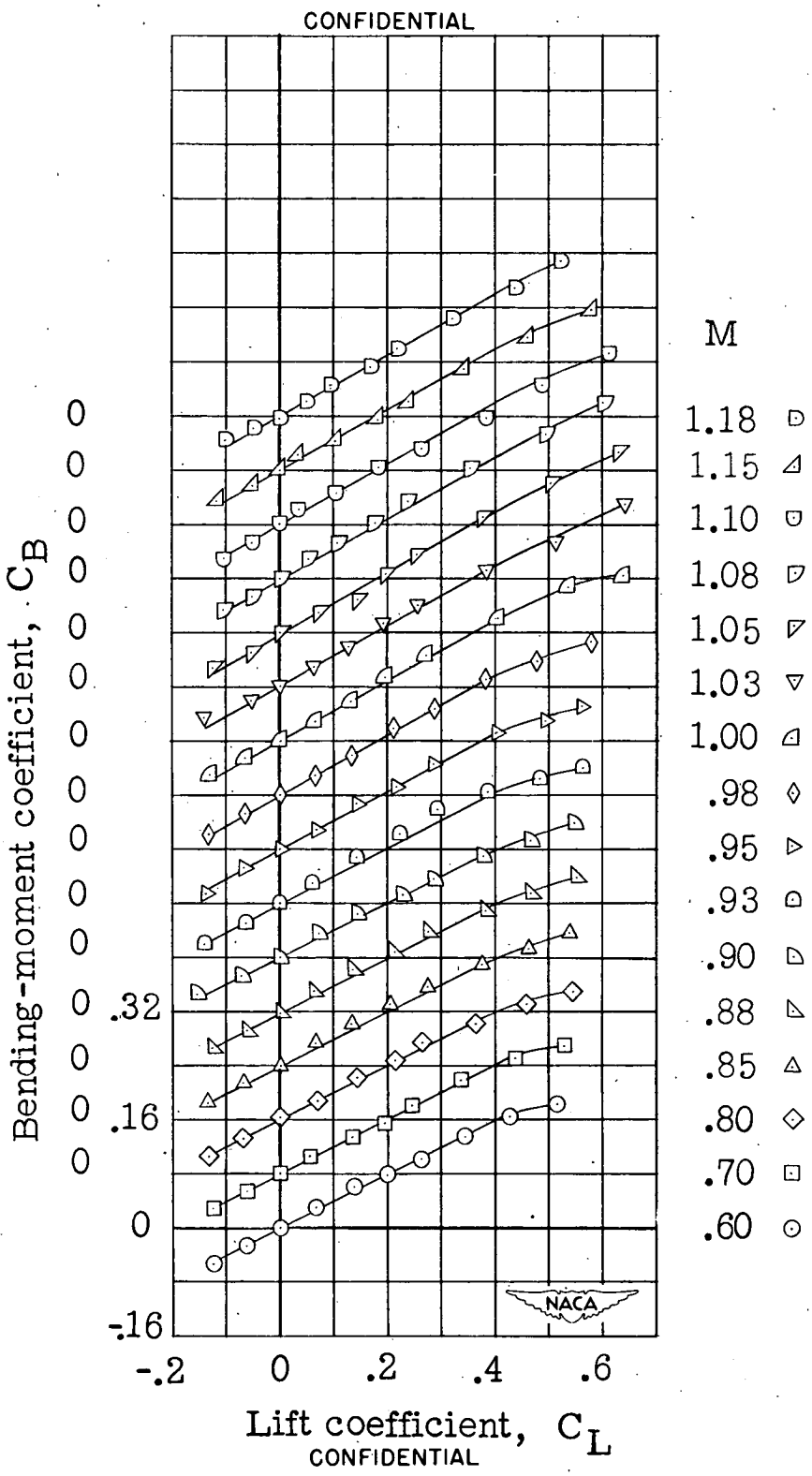

Figure 7.– Concluded.

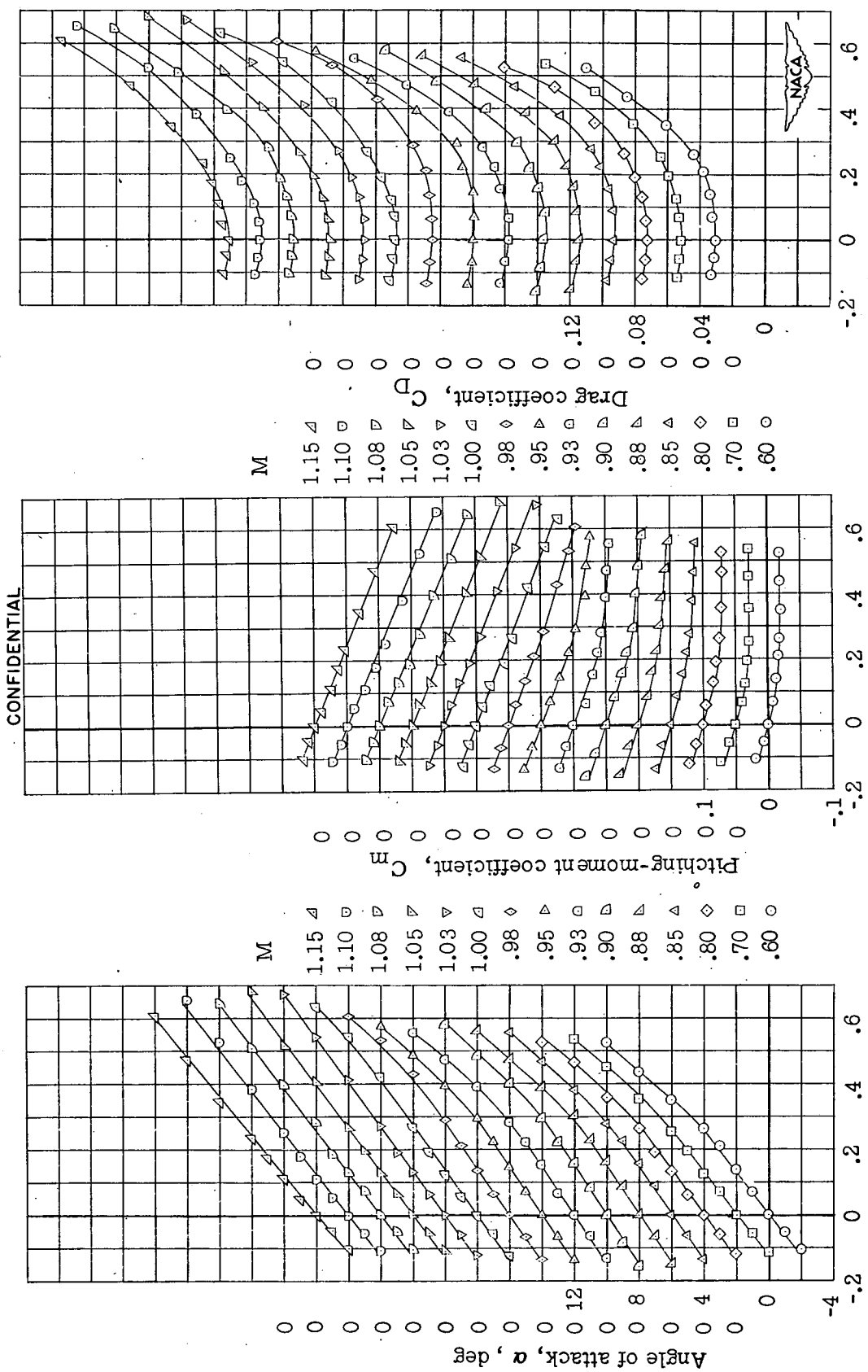

Figure 8.- Wing-fuselage aerodynamic characteristics for delta-wing model with leading edge swept back 45°, aspect ratio 4, and NACA 65A006 airfoil.

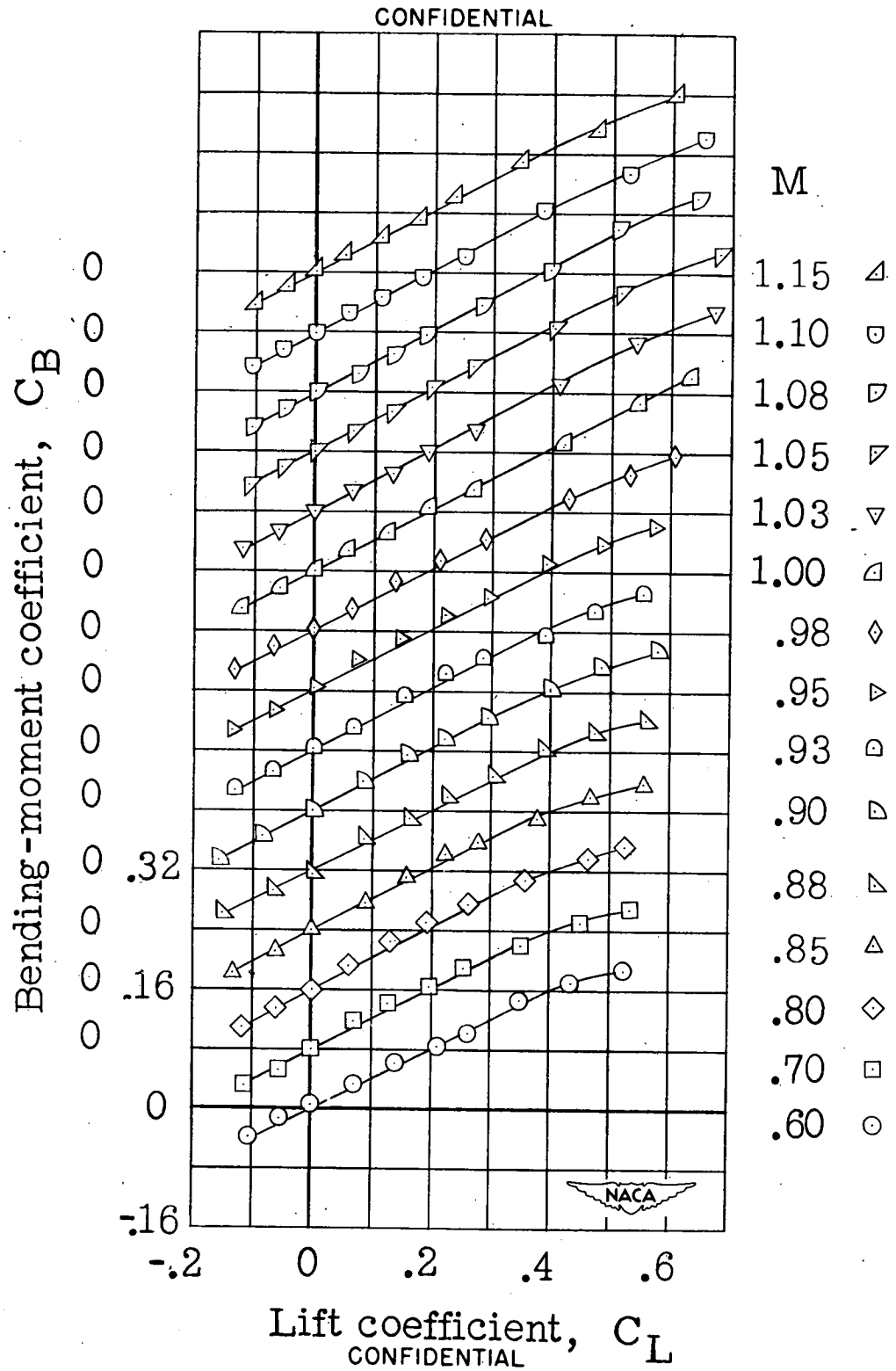

Figure 8.– Concluded.

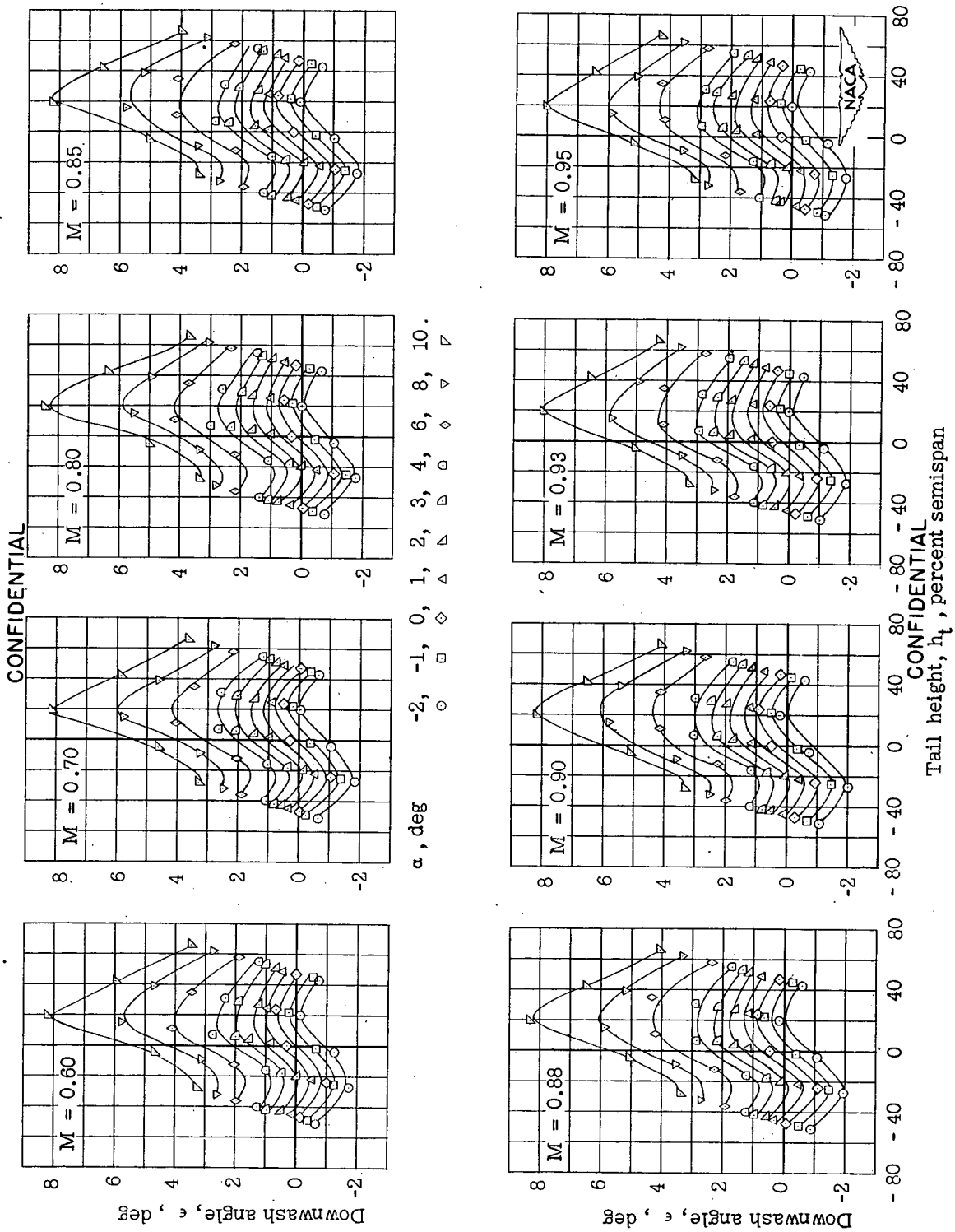

Figure 9.- Effective downwash angles in region of tail plane for delta-wing model with leading edge swept back 45°, aspect ratio 4, and NACA 65A006 airfoil. Wing alone.

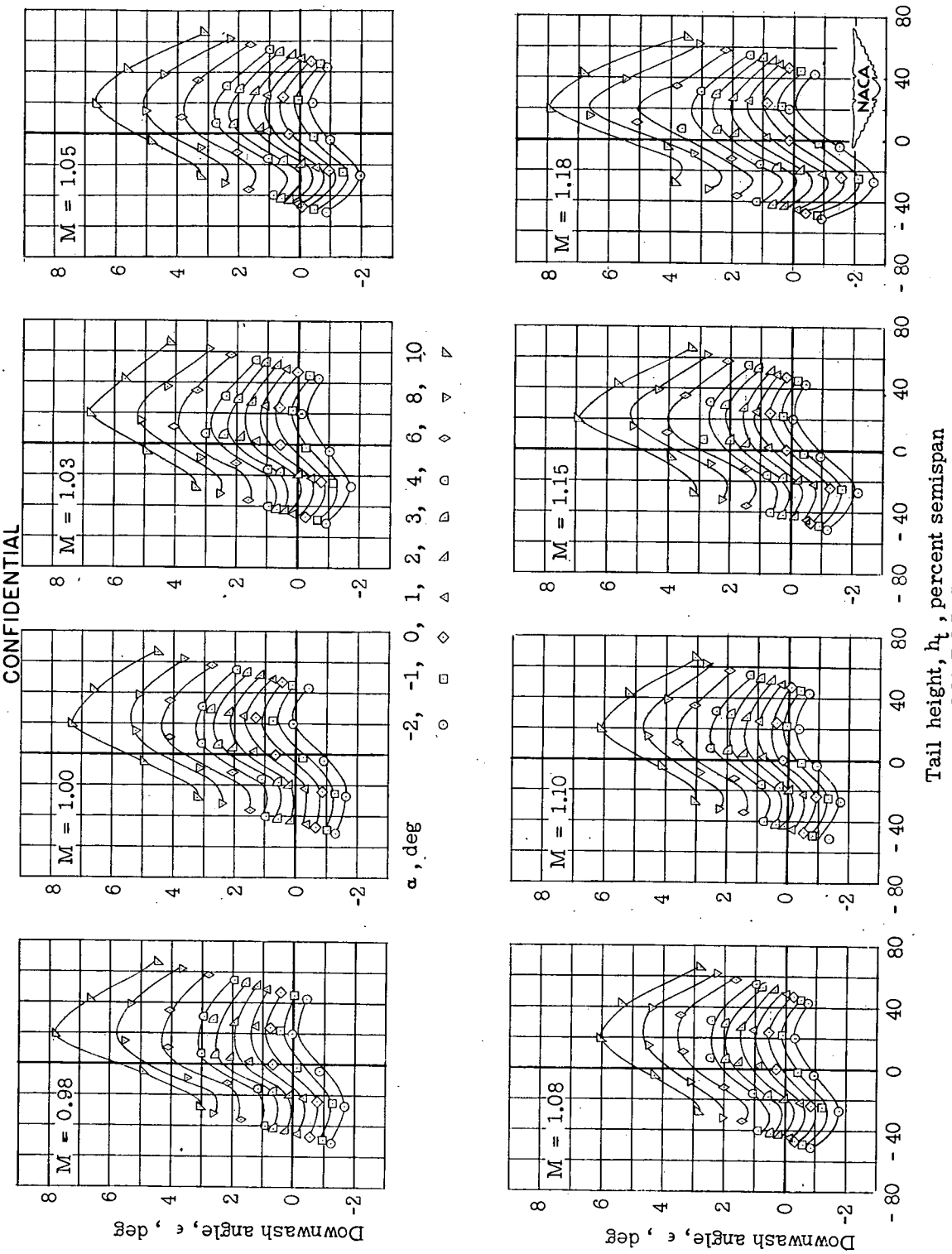

Figure 9.- Concluded.

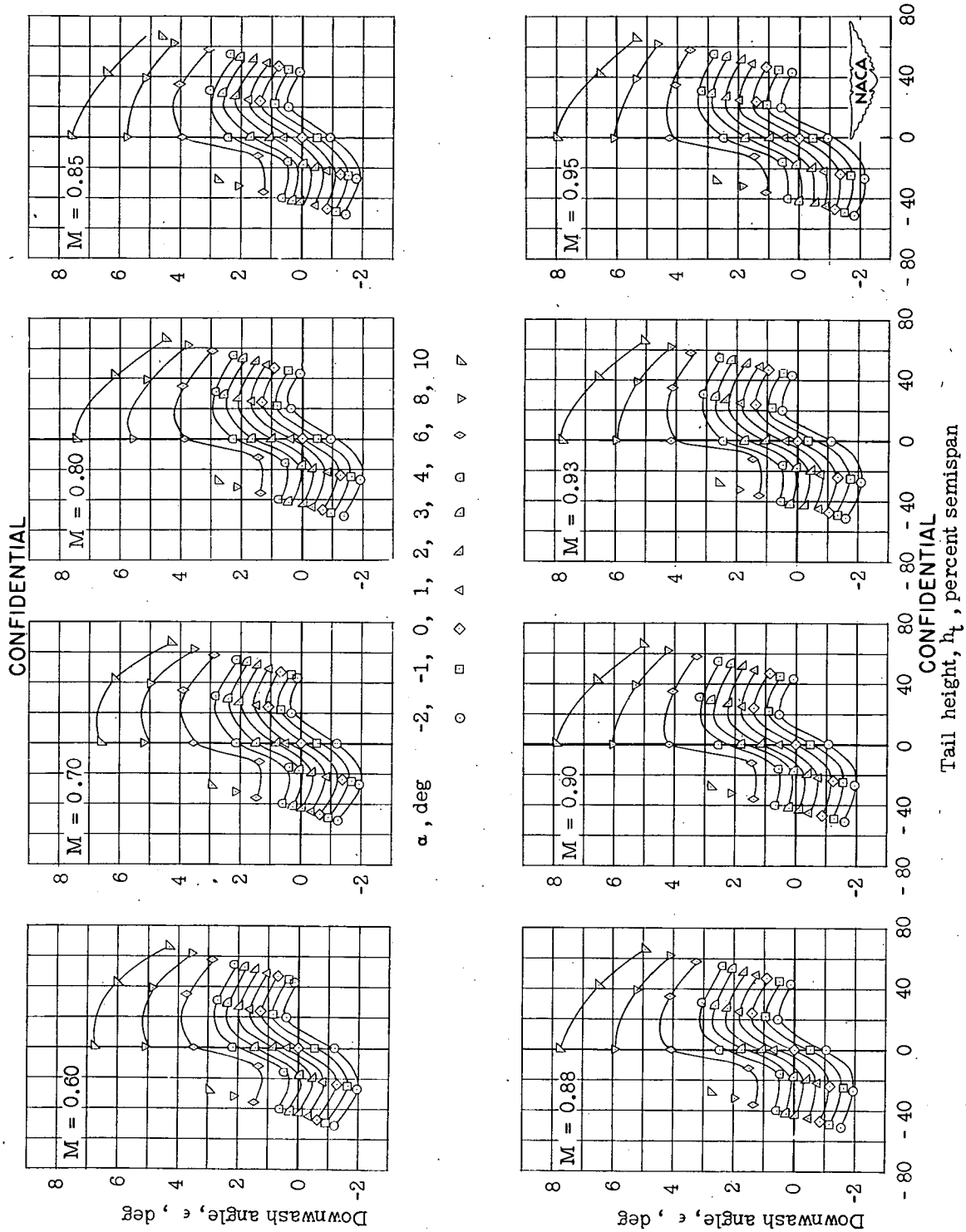

Figure 10.- Effective downwash angles in region of tail plane for delta-wing model with leading edge swept back 45°, aspect ratio 4, and NACA 65A006 airfoil. Wing fuselage.

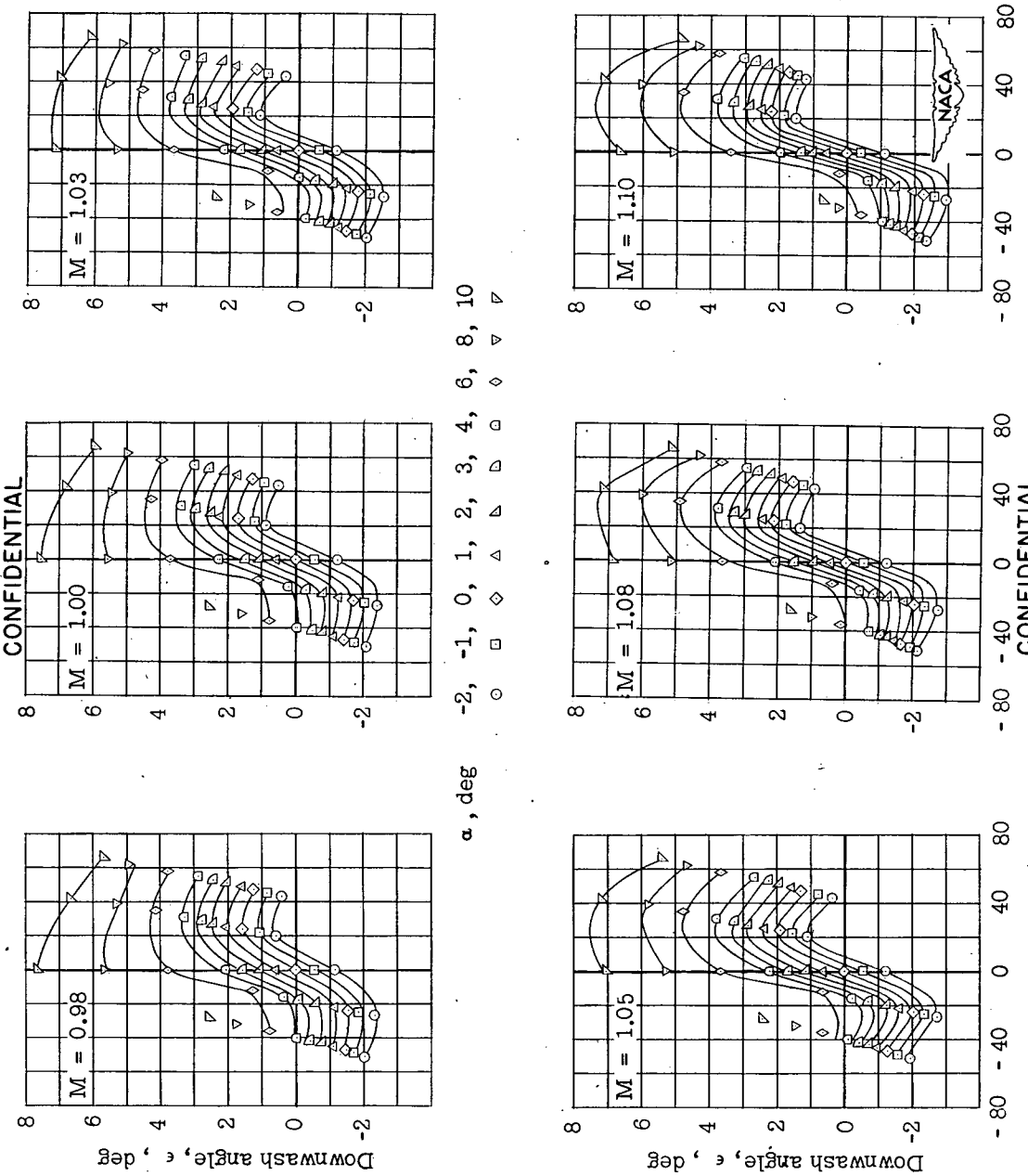

Figure 10.- Concluded.

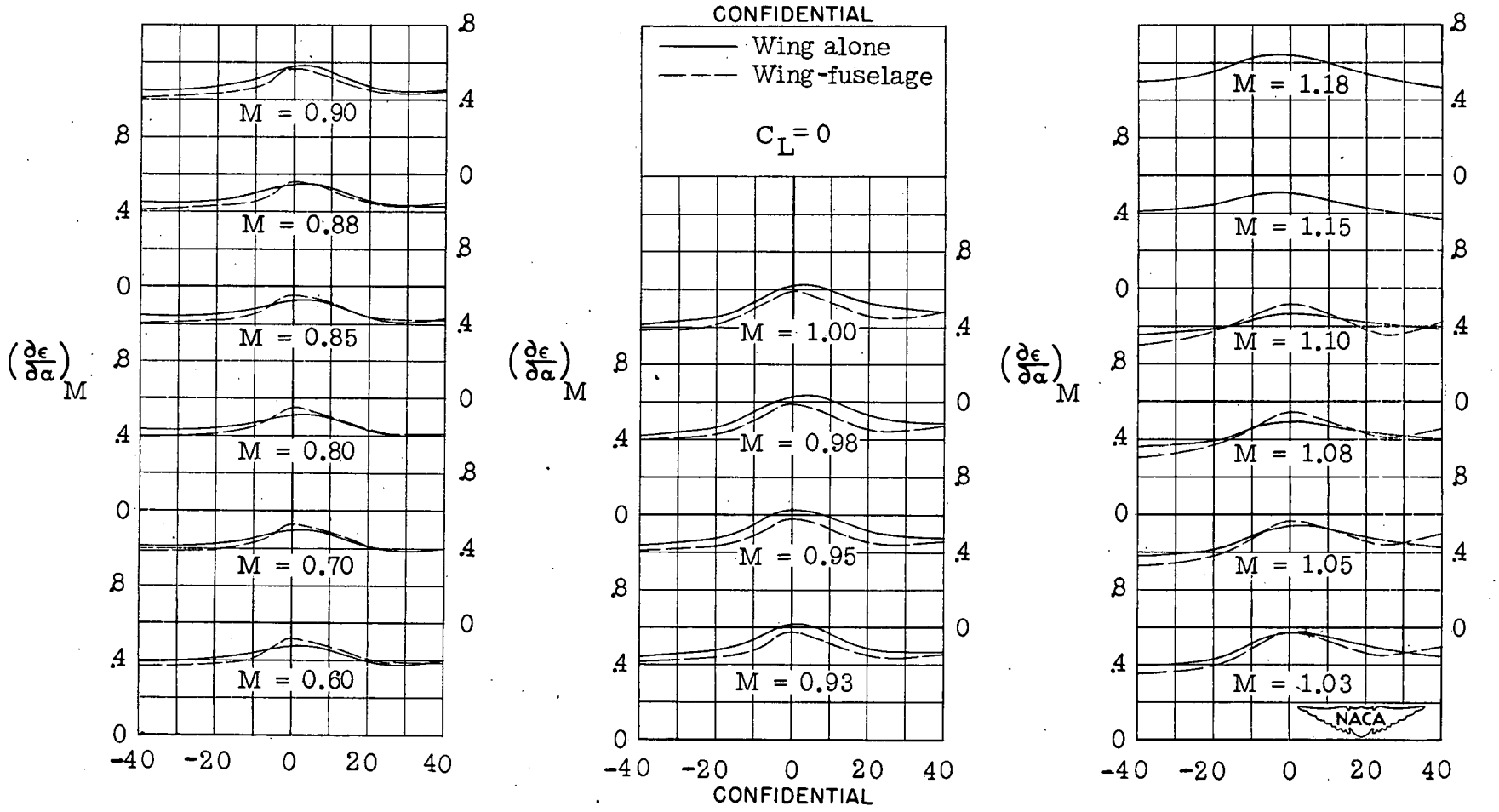

Figure 11.— Variation of downwash gradient with tail height and Mach number for delta-wing model with leading edge swept back 45°, aspect ratio 4, and NACA 65A006 airfoil.

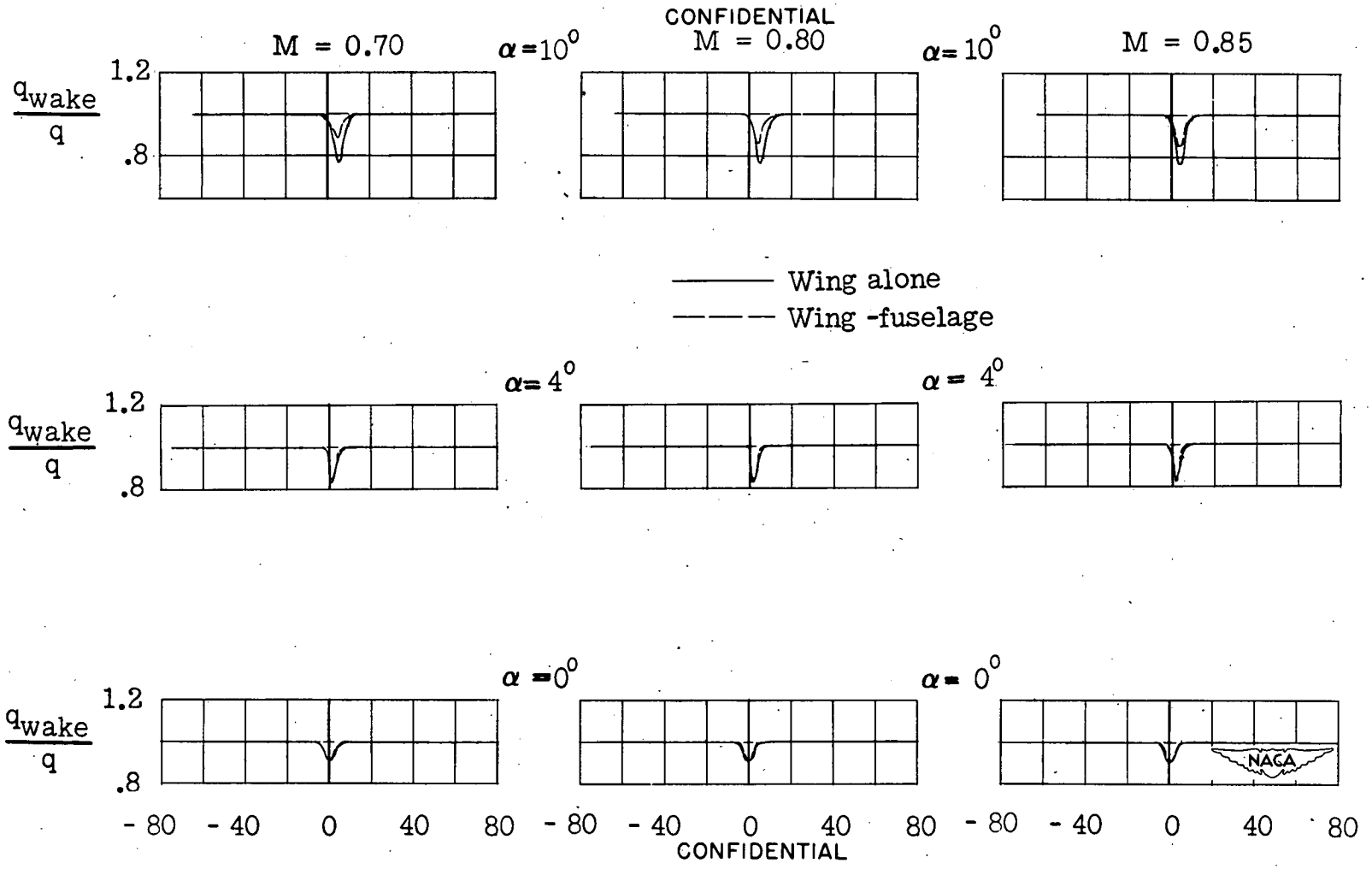

Figure 12.– Dynamic–pressure surveys in region of tail plane for delta–wing model with leading edge swept back 45°, aspect ratio 4, and NACA 65A006 airfoil.

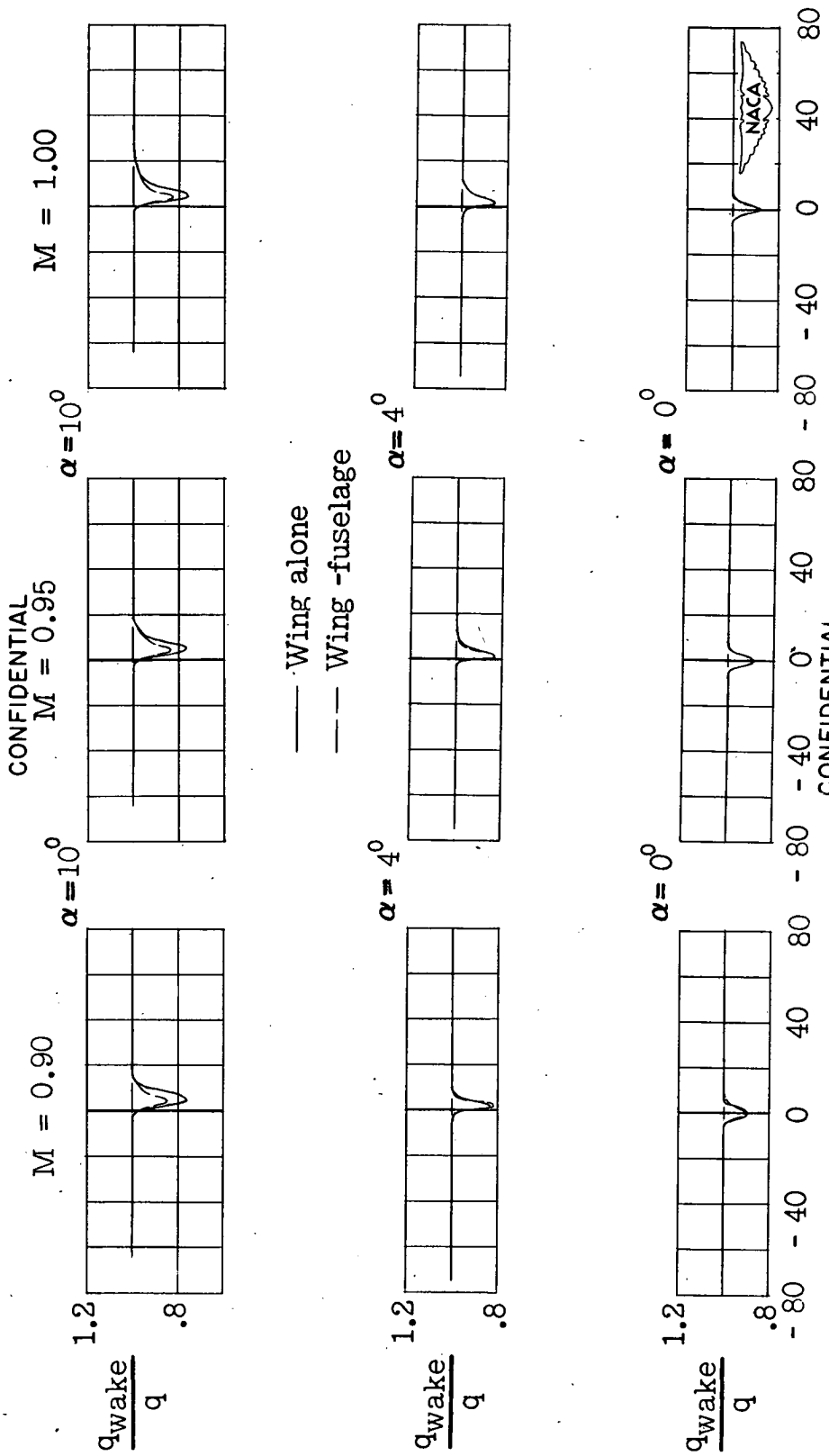

Figure 12.- Continued.

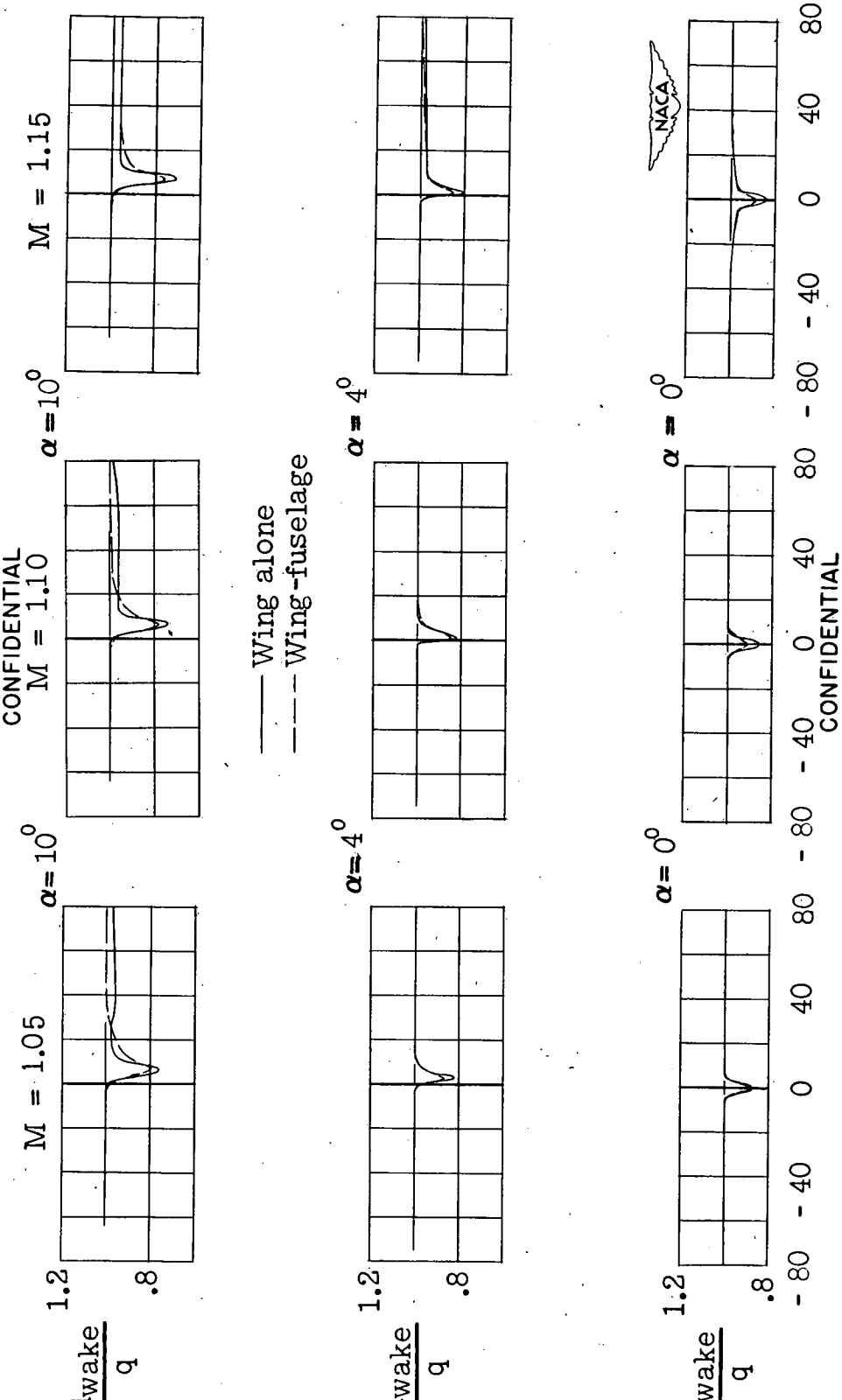

Figure 12.- Concluded.

CONFIDENTIAL

——Wing alone

——Wing -fuselage

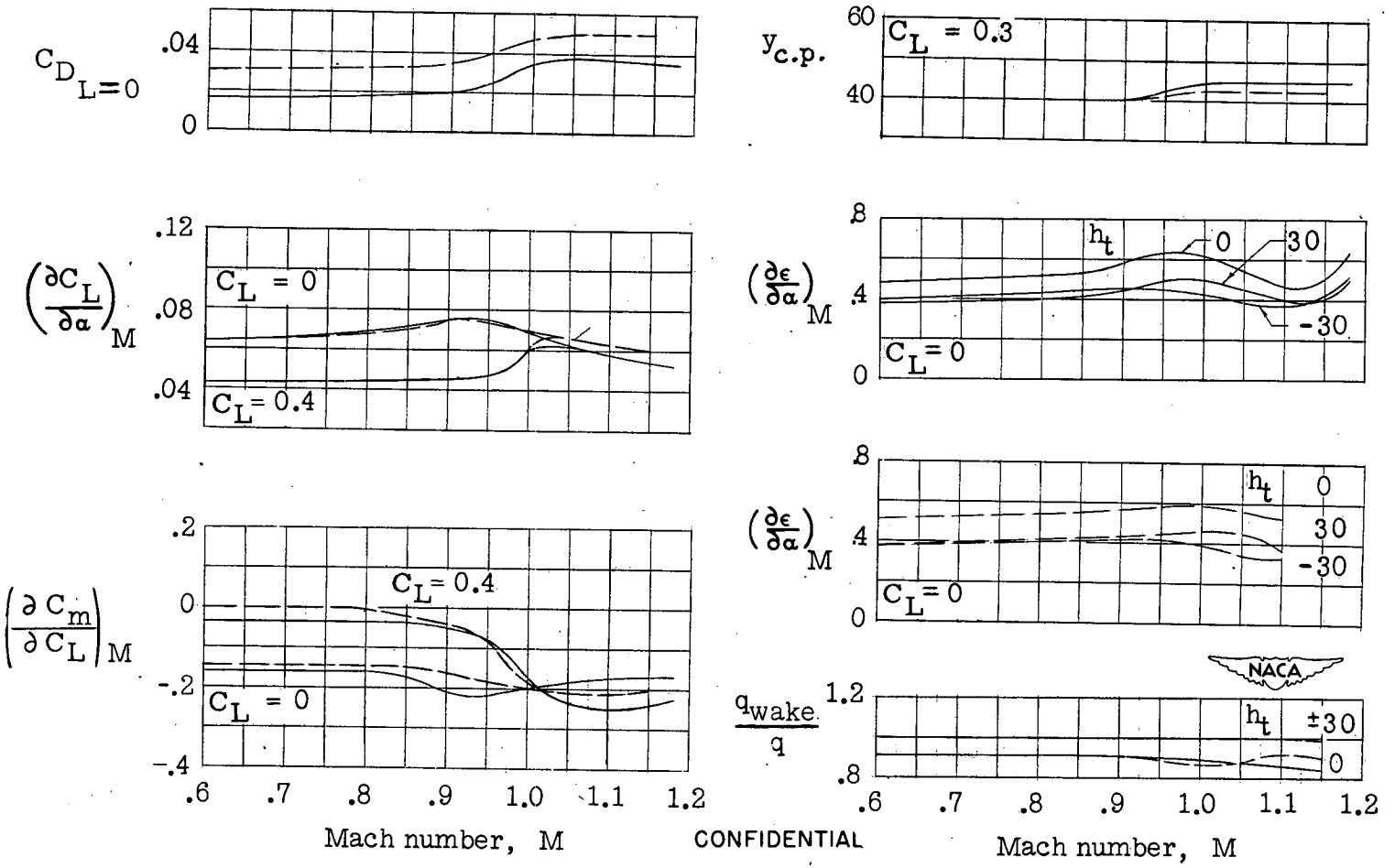

CONFIDENTIAL

Figure 13.– Summary of aerodynamic characteristics for delta–wing model with leading edge swept back 45°, aspect ratio 4, and NACA 65A006 airfoil.